Aggregation and Induced Chirality of an Anionic *meso*-Tetraphenylsulfonato Porphyrin (TPPS) on a Layer-by-Layer Assembled DNA/PAH Matrix

Siguang Jiang and Minghua Liu*

CAS Key Laboratory of Colloid and Interface Science, Center for Molecular Science, Institute of Chemistry, Chinese Academy of Sciences, Beijing 100080, People's Republic of China

Received: September 28, 2003; In Final Form: January 7, 2004

The aggregation and induced chirality of an anionic *meso*-tetraphenylsulfonato porphyrin (TPPS) on a layer-by-layer assembled deoxyribonucleic acid/poly(allylamine hydrochloride) (DNA/PAH) film were investigated. It was found that TPPS could directly penetrate into a DNA/PAH film and be assembled into both H-aggregates and J-aggregates. Both of the aggregates showed strong induced circular dichroism (CD) in the film. On the other hand, TPPS could also penetrate into the DNA/PAH film through the help of a cationic *meso*-tetrakis-(4-*N*-methylpyridyl) porphyrin (TMPyP), as a spacer. In this case, J-aggregates formed in the DNA/PAH matrix and induced chirality was also observed. The induced chirality of the TPPS J-aggregate followed the DNA chirality, in the presence of TMPyP; however, an opposite induced chirality was observed in the absence of TMPyP. Atomic force microscopy images showed nanorods on the surface of DNA layer in both cases, which were composed of H-type and/or J-type aggregates of TPPS. The mechanism of the formation of the opposite induced CD signals was discussed.

1. Introduction

Chiral supramolecular assemblies have been drawing much attention, because of their applications in asymmetric catalysis,[1] liquid crystals,[2,3] and potential unique properties, such as nonlinear optical materials.[4,5] Although chiral molecules are widely used to fabricate the chiral assemblies,[6−9] it has been proven to be very effective to take advantage of the induced chirality phenomenon, in which the chirality of an achiral molecule can be induced in a chiral template.[10−14] A chiral environment, such as the cavity of cyclodextrin, is an important host to induce the chirality of small molecules.[15,16] Biological substances such as proteins, nucleic acids, and polypeptides serve as a class of important chiral templates and the induced chirality in these matrixes has been widely investigated.[10,12,13] Among the biological substances, deoxyribonucleic acid (DNA) is particularly interesting. DNA has a unique double-helical structure, which is one of the most interesting supramolecular architectures, and it has a large amount of phosphate groups and ribose units on its helical backbone and shows the chirality and typical properties of a polyanion. In addition, DNA has a special property of intercalation, in which many dye molecules can be bound to DNA and exhibit induced chirality.[12,17] However, DNA is water-soluble and most of these properties are realized in aqueous solutions. To functionalize DNA, it is important to immobilize the DNA into film or other states. Previously, through a layer-by-layer (LbL) deposition with poly-(allylamine hydrochloride) (PAH), we have found that DNA could be uniformly assembled into a water-insoluble ultrathin film. In addition, the DNA/PAH film could be used as a matrix to incorporate a cationic dye, such as *meso*-tetrakis-(4-*N*-methylpyridyl) porphyrin (TMPyP), and the chirality of TMPyP was also induced in the film.[18] In a continuation work on the interaction between DNA and dyes, we have found that, although it is an anionic dye, *meso*-tetrakis-(4-sulfonatophenyl) porphyrin (TPPS) experiences repulsion with DNA in aqueous solution, and the addition of a cationic TMPyP could cause interaction between DNA and TPPS.[19] In this paper, we extended our research in the film system. It was surprising to observe that TPPS could directly interact with the DNA/PAH film and showed a strong induced chirality. If a TMPyP-intercalated DNA/PAH was used as a ternary matrix, TPPS could also interact with DNA through the TMPyP as a spacer. Interestingly, the induced chirality of the TPPS J-aggregate followed the DNA chirality in the presence of TMPyP; however, an opposite induced chirality was observed in the absence of the TMPyP. So far, much research has been done on the interaction between DNA and cationic dyes, and little has been reported on the interaction between DNA and anionic dyes.[20] Here, we report an example of the interaction between an anionic dye and DNA in film and show an opposite induced chirality of the same dye in the film.

2. Experimental Section

2.1. Materials. Sodium salt of DNA from a salmon spermary was purchased from Wako Pure Chemical Industries, Ltd. The concentration of DNA was obtained via absorption measurement using $\epsilon = 1.31 \times 10^4\ M^{-1}\ cm^{-1}$ at the maximum near a wavelength of 260 nm (i.e., DNA concentrations are reported in molar base pairs).[21] PAH (average molecular weight of 8500−11000, Nippon Boseki) was used without further purification. Water-soluble cationic porphyrin TMPyP and anionic porphyrin TPPS were purchased from Dojindo Laboratories. Their structures are shown in Chart 1. In the experimental process, deionized Millipore-Q water (18.2 MΩ cm) was used.

2.2. Preparation of the Films. A quartz plate was cleaned, using mixed chromic acid, overnight and used to assemble the DNA films. It was coated first with PAH by immersing the plates into 1 mg/mL of a PAH aqueous solution (pH 2.4) for 10 min. After the plates were removed, rinsed with distilled

* Author to whom correspondence should be addressed. E-mail: liumh@iccas.ac.cn.

10.1021/jp036886l CCC: $27.50
Published on Web 02/05/2004

CHART 1. Materials Used in This Study

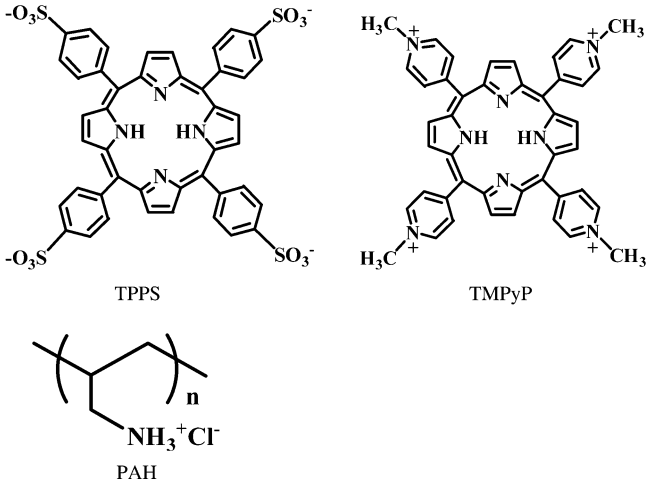

water, and dried with nitrogen, the substrate was immersed into 1 mM DNA aqueous solution for 10 min and then rinsed and dried as described previously. An LbL assembly of DNA/PAH film can be obtained by repeating the aforementioned procedures. TPPS aqueous solution (1mM), adjusted to a pH value of 2.4 with diluted HCl, was used as an immersing solution and the TMPyP immersing solution was adjusted to pH 9.0 with diluted NaOH in this paper. TPPS-incorporated DNA/PAH film was fabricated by immersing the DNA/PAH film into the TPPS solution for various time intervals. In the case of TMPyP as a spacer, DNA/PAH film was first immersed into TMPyP solution for 10 min and then into TPPS solution for a certain time. In regard to atomic force microscopy (AFM) measurements, mica was used as the substrates on which three DNA/PAH bilayers were deposited and the outermost layer was DNA. The films were immersed in TPPS solution for 5 min to obtain TPPS-incorporated DNA/PAH film. In the case of TMPyP, the films were first immersed into TMPyP solution for 1 min and then immersed in TPPS solution for 5 min.

2.3. Instruments. UV−Vis spectra of the films were recorded on a JASCO model UV-530 spectrophotometer and circular dichroism (CD) spectra were recorded (JASCO, model J-810). In the process of CD spectral measurement, the LbL films were placed perpendicular to the light path and rotated within the film plane, to avoid the polarization-dependent reflections and eliminate the possible angle dependence of the CD signals.[22,23] AFM (Digital Instruments, model Nanoscope III A) was used to visualize the surface morphology of the films with a tapping mode.

3. Results and Discussions

3.1. Interaction of TPPS and DNA/PAH Film. 3.1.1. UV−Vis Spectra. Previously, we have found that the LbL assembled DNA/PAH film was insoluble in water. By immersing the DNA/PAH film into a neutral aqueous solution that contained dyes such as TMPyP and ethidium bromide, the dyes could be incorporated into the DNA/PAH film and exhibited intercalation with DNA film.[18] However, all the loaded dyes are cationic, because DNA is an anionic polymer. To determine if the anionic dye could interact with DNA film, we have tried to immerse the DNA/PAH film into an aqueous TPPS solution. Surprisingly, the colorless DNA/PAH film became green after it had been immersed for a certain time. This process was monitored using UV−Vis spectroscopy. Figure 1 shows the UV−Vis spectral changes when DNA/PAH film was immersed into the aqueous

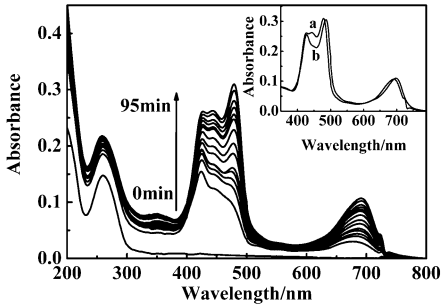

Figure 1. UV−Vis spectra of TPPS penetrated into DNA/PAH film after different time intervals. Inset shows the change of spectra (a) before and (b) after the film was placed in air overnight.

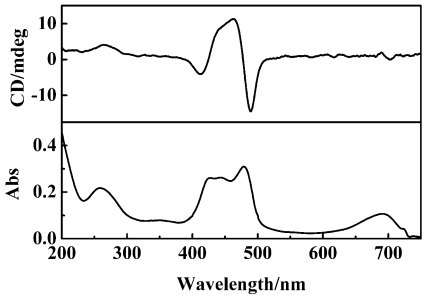

Figure 2. Circular dichroism (CD) (top) and UV−vis (bottom) spectra of TPPS-incorporated DNA/PAH film.

TPPS solution for different time intervals. Four absorption bands are observed, at 427, 443, 479, and 691 nm, which can be attributed to the B-bands of the H-aggregate, the diprotonated monomer, and the J-aggregate and the Q-band of the J-aggregate, respectively. This indicates that, when TPPS was loaded into the DNA/PAH matrix, the TPPS underwent aggregation in the film and formed both H- and J-aggregates. In various time intervals, the relative intensity of the four bands was different. There was an obvious tendency for the J-band to increase its intensity greatly as the immersion time increased. The incorporation of TPPS into the DNA/PAH film was saturated within 100 min, as verified from the UV−Vis absorption spectra. When the DNA/PAH film saturated with TPPS was put in the air overnight at room temperature, only two main peaks—at 427 and 486 nm—were observed in the Soret band (see inset of Figure 1). This indicates that the monomer can change into the aggregates and both the H- and J-aggregates are more stable than the monomer in the film. In addition, from our UV−Vis spectra, the H-aggregate absorbance intensity clearly seems to be much higher than that of the J-aggregate at the beginning of the loading, which suggests that, in DNA/PAH films, the formation of the H-aggregate happens more easily than that of the J-aggregate when the amount of TPPS is low. However, as the loading time increased, the absorbance of the J-aggregate increased faster than that of the H-aggregate, because the former is much more stable than the latter.

3.1.2. Circular Dichroism (CD) Spectra. It is well-known that DNA is a chiral polymer, and some cationic dyes are reported to show induced chirality in the DNA matrix.[10,17] To determine if the penetrated TPPS in the DNA/PAH film has any interaction with DNA, we have measured the CD spectra of TPPS-incorporated DNA/PAH films, as shown in Figure 2. Interestingly, in addition to a typical CD signal that is ascribed to DNA at the short-wavelength region, there is a strong induced CD signal in the visible region, which corresponds to the aggregates absorption of TPPS in Soret and Q-bands. The CD signal in the Soret band region can be regarded as the composite of two components. One is ascribed to the J-aggregate, where positive

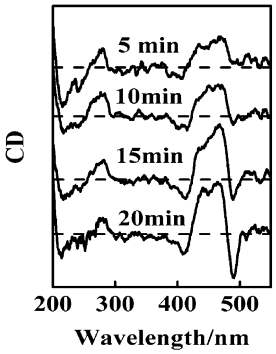

Figure 3. CD spectra of DNA/PAH multilayer films for different loading times in a 1 mM TPPS aqueous solution at pH 2.4. (Dashed lines show the zeros of the respective CD spectra.)

and negative Cotton effects are observed at 462 and 489 nm, respectively, with a crossover at 479 nm. The other can be assigned to the H-aggregate of TPPS, where negative and positive Cotton effects appear at 412 and 439 nm, respectively, with a crossover at 426 nm. In addition, the Q-band also shows an exciton coupling. The sign of the split CD band at 691 nm is very prominent and matches that of the CD band at the J-aggregate, which strongly supports the formation of chiral J-aggregates.[24−26] The CD sign of the H- and J-bands are just opposite, which suggests that the electronic transition dipole moments of the H- and J-aggregates are vertical. This observation indicates that the interaction of DNA and TPPS not only makes the TPPS J- and H-aggregates exhibit induced CD, but the electron transition dipole moments also are vertical to each other, which is in accordance with the literature report.[27]

We also measured the CD spectral change, relative to different loading times, as shown in Figure 3. The Cotton effect of DNA at short wavelengths clearly did not change with loading time and always exhibited B-form. While the CD spectra of the J-aggregate showed a signal without split, the H-aggregate showed a split Cotton effect at the beginning of the loading. The exciton coupling observed in the H-aggregate suggests that not only was the H-aggregate formed easily but also adjacent H-aggregates experienced great interaction with each other in the presence of DNA, which was accordance with the UV−Vis spectra extensively. The CD amplitude of both aggregates increased as the loading time increased, although the increase in the CD amplitude of the J-aggregate was much faster than that of the H-aggregate. It is well-known that the J-aggregate is more stable than the H-aggregate and the formation of the J-aggregate can decrease the energy of the entire system. This indicated that the H-aggregate was kinetically favored, whereas the J-aggregate was thermodynamically preferred.

3.1.3. Atomic Force Microscopy (AFM) Measurements. To clarify the interaction between TPPS and DNA further, AFM was performed to observe the differences in the surface morphology. The morphology of the three bilayers of DNA/PAH film, whose outermost layer is DNA, was visualized by AFM on mica, as shown in Figure 4A. The DNA/PAH film is relatively uniform and flat, with an average roughness of ∼0.493 nm in a region with dimensions of 2 μm × 2 μm. However, after the film was immersed into the TPPS aqueous solution for 5 min, the surface morphology of the film underwent great change, and many nanorods appeared on the surface, as shown in Figure 4B. It has been reported that both aggregates of TPPS have pyrrolic rings in the porphinato macrocycle that are alternately ruffled up and down: one can be viewed as forming a slipped card-deck structure, with the negative charges on the periphery of one molecule overlapping the positive charges in the center of the neighboring porphyrin, and the other can be viewed as a stacked card-deck arrangement, with phenyl and macrocycle groups almost directly above and below each other.[28,29] According to these observations, it is reasonable to say that the nanorods are composed of J- and H-aggregates of TPPS. This result was strong evidence that the interaction of TPPS and DNA caused the deposition of TPPS on the DNA surface in the J- and H-aggregates.

It is reported that TPPS can easily form chiral J-aggregates under certain conditions and the chirality of the TPPS aggregate followed the chiral molecules, such as lysine or polylysine.[30] However, in all these cases, cationic chiral molecules were used. In our case, the chiral molecule is anionic DNA. Although no interaction between DNA and TPPS was observed in solution, induced CD spectra of TPPS H- and J-aggregates were detected in the DNA/PAH film. This can be explained as follows. LbL film is regarded as having no clear interface and the two types of polymers are interpenetrated. Thus, the space in the DNA/PAH film can be regarded as a chiral environment. Therefore, both of the aggregates of TPPS in this environment exhibit induced chirality. Moreover, because the film was formed in an acidic environment, a hydrogen bond might be formed between the phosphate and the inner hydrogen of TPPS.[20,31] This could be an important reason for the induced chirality of TPPS aggregates. In addition, DNA has a double helical structure. When it formed a polyion complex with PAH, the major and minor grooves of the DNA can be vacant and, thus, leave space for the penetration of both cationic and anionic dyes. We have investigated the interaction between TPPS and other LbL assembled polymer films, such as poly(sodium 4-styrenesulfonate)/PAH and poly(acrylic acid)/PAH film. No induced chirality was detected in either the H- or J-aggregates, although TPPS could penetrate into the films.

3.2. Interaction of TPPS and DNA/PAH Film in the Case of the TMPyP Spacer. Previously, we have reported that TMPyP could easily penetrate into DNA/PAH film when the film was immersed into TMPyP aqueous solution. We now observe that TMPyP-incorporated DNA/PAH film can further incorporate the TPPS, by immersing the film into TPPS solution, as shown in Figure 5.

A narrow and sharp absorption band was observed at 489 nm, with a slight increase and shift on the band of 440 nm. The band at 489 nm can be regarded as being due to the J-aggregation of TPPS in the film, which can be further verified from the Q-band at 705 nm. The band of 440 nm might be attributed to the overlap of several components. The DNA/PAH/TMPyP/TPPS film exhibited a strong induced CD spectrum in the visible region, as shown in Figure 6. The ICD spectrum of the film can be regarded as a composite of three exciton couplets in the Soret band. One couplet is due to the TPPS H-aggregate, which shows the negative Cotton effect at 420 nm; the second couplet might be due to the TMPyP−TPPS complex, which shows a positive Cotton effect at 445 nm;[19] and the third couplet is due to the TPPS J-aggregate, which shows a split band with a crossover at 489 nm. It is reported that, although TPPS and DNA showed no direct interaction in solution, the addition of TMPyP into the solution can induce the chirality of TPPS where TMPyP acts as a spacer.[19,32] This could be true in our film. When TPPS penetrates into a TMPyP-incorporated DNA/PAH film, TPPS not only forms a complex with TMPyP but also can form J-aggregates on the positively charged TMPyP. Therefore, we can observe the induced CD signal at the TPPS−TMPyP complex and TPPS J-aggregation bands.

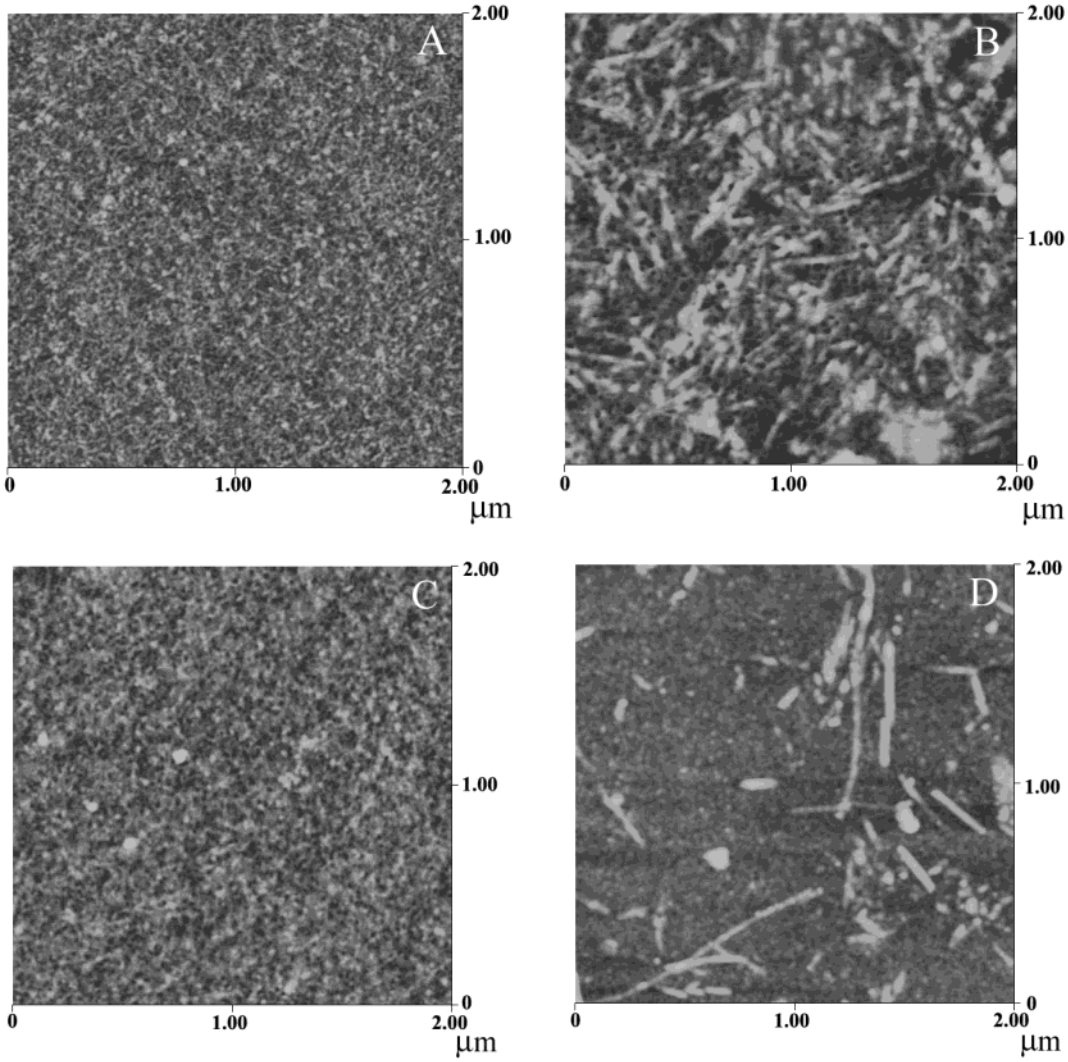

Figure 4. AFM photomicrographs of three bilayers of film on mica: (A) the DNA/PAH film; (B) the DNA/PAH/TPPS film; (C) the DNA/PAH/TMPyP film; and (D) the DNA/PAH/TMPyP/TPPS film. The outermost layer is DNA.

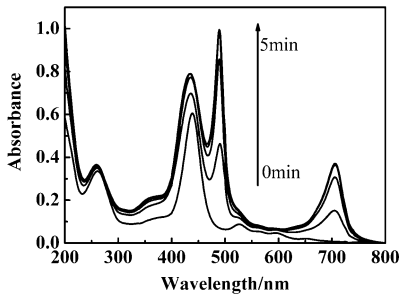

Figure 5. UV−Vis spectra of TPPS penetrated into TMPyP-incorporated DNA/PAH film after different time intervals.

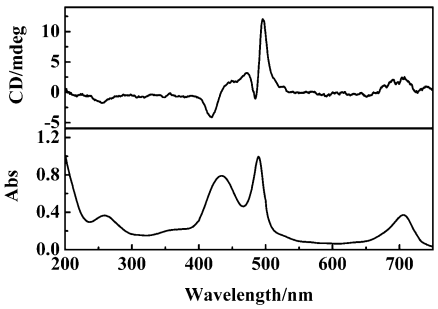

Figure 6. CD (top) and UV−Vis (bottom) spectra of TPPS penetrated into TMPyP-incorporated DNA/PAH film.

We also measured the AFM images of DNA/PAH/TMPyP and DNA/PAH/TMPyP/TPPS films, as shown in Figure 4C and 4D, respectively. In regard to DNA/PAH/TMPyP film, the morphology did not change significantly, in comparison to that of the DNA/PAH film. The reason is that TMPyP molecules intercalated or bonded in the DNA layer and do not assemble into aggregates. For DNA/PAH/TMPyP/TPPS film, a similar nanorod structure is also observed, as in the case of DNA/PAH/TPPS film. However, compared to the nanorods on DNA/PAH/TPPS film, the nanorods on the DNA/PAH/TMPyP/TPPS film are longer. All these morphological changes are in accordance with the aforementioned UV−Vis spectra.

When comparing the CD spectra of TPPS in DNA/PAH and DNA/PAH/TMPyP films, the CD sign of the J couplet of TPPS interestingly is just opposite in the two films in both the Soret band, at ∼490 nm and the Q-band, at ∼701 nm. Such opposite CD signs of the TPPS J-aggregate in the two different cases could be explained as illustrated in Figure 7. In the case of TMPyP-incorporated DNA/PAH film, TMPyP was intercalated into the base pairs of the DNA, which was verified by the CD spectra of the DNA/PAH/TMPyP film. When TPPS was added into the system, TPPS could form a heterocomplex with TMPyP, because of the strong interaction between TMPyP and TPPS. This was reported in aqueous solution in our previous work.[19] This also occurred in the film, as verified from our UV−Vis

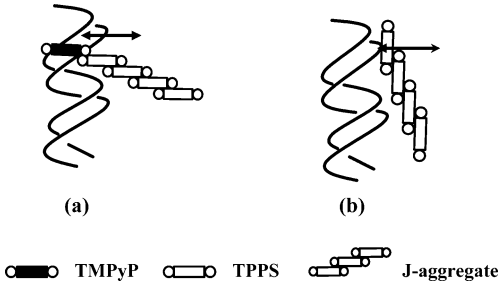

Figure 7. A plausible interaction mode between TPPS and DNA in the (a) presence and (b) absence of TMPyP in the DNA/PAH films. Arrows indicate the transition moment of the interaction. TMPyP was intercalated into the DNA base pairs.

and CD spectra for the DNA/PAH/TMPyP/TPPS film. Moreover, when excess TPPS penetrated into the TMPyP-incorporated DNA/PAH film, TPPS could form a homo J-aggregate on the TMPyP. In this case, the chirality of TPPS will follow the induced chirality of TMPyP. Because the induced chirality of TMPyP followed the chirality of DNA, the heterocomplex between TMPyP and TPPS and the J-aggregate of TPPS in this case would also follow the chirality of DNA. Here, TMPyP served as a spacer and the chirality of DNA was imprinted to TPPS through TMPyP. In the case of TPPS/DNA/PAH film, the ternary system was fabricated in an acidic environment of pH 2.4. In this condition, TPPS could be protonated in its inner nitrogen. Therefore, it is possible for DNA to attach to the inner protonated nitrogen of TPPS, as shown in Figure 7b. A similar interaction mode between DNA and TPPS, using the inner nitrogen, was suggested by Purrello et al., who related the interaction between DNA and porphyrins,[20] although, presently, we cannot get direct experimental support. In the case of TMPyP as a spacer, the transition moment was in the plane of the macrocyclic ring of porphyrin, whereas, in the absence of TMPyP, the direct interaction between DNA and the inner protonated nitrogen caused the interaction transition moment in a vertical direction to the macrocyclic ring, as shown in Figure 7. Therefore, we could observe the opposite CD signals in the J-bands in the two cases.

4. Conclusion

In conclusion, it was suggested that a dianionic *meso*-tetraphenylsulfonato porphyrin (TPPS) could directly penetrate into a deoxyribonucleic acid/poly(allylamine hydrochloride) (DNA/PAH) film or through the help of a cationic *meso*-tetrakis-(4-*N*-methylpyridyl) porphyrin (TMPyP). In both cases, J-aggregates of TPPS were formed and induced chirality was observed. Although the induced chirality of TPPS followed the DNA chirality in the presence of TMPyP as a spacer, an opposite chirality was observed in the absence of the TMPyP, which could be attributed to a different interaction mode of TPPS with DNA. In the presence of TMPyP, TPPS was supposed to interact with DNA through the TMPyP as a spacer. In the absence of TMPyP, TPPS was supposed to interact with DNA via a hydrogen bond or other interactions. These results will be helpful in designing chiral materials.

Acknowledgment. This work was supported by the Outstanding Youth Fund (No. 20025312), the National Science Foundation of China (No, 20273078), the Major State Basic Research Development Program (G2000078103, 2002CCA-03100), and the Fund of the Chinese Academy of Sciences.

References and Notes

(1) Nimri, S.; Keinan, E. *J. Am. Chem. Soc.* **1999**, *121*, 8978.
(2) van Nostrum, C. F.; Bosman, A. W.; Gelinck, G. H.; Picken, S. J.; Schouten, P. G.; Warman, J. M.; Schouten, A. J.; Nolte, R. J. M. *J. Chem. Soc. Chem. Commun.* **1993**, 1120.
(3) Ribo, J. M.; Crusats, J.; Sagues, F.; Claret, J.; Rubires, R. *Science* **2001**, *292*, 2063.
(4) Verbiest, T.; Van Elshocht, S.; Kauranen, M.; Hellemans, L.; Snauwaert, J.; Nuckolls, C.; Katz, T. J.; Persoons, A. *Science* **1998**, *282*, 913.
(5) Lin, W.; Ma, L.; Wang, Z. *J. Am. Chem. Soc.* **1999**, *121*, 11249.
(6) Hanessian, S.; Gomtsyan, A.; Simard, M.; Roelens, S. *J. Am. Chem. Soc.* **1994,** *116*, 4495.
(7) Engelkamp, H.; Middelbeek, S.; Nolte, R. J. M. *Science* **1999**, *284*, 785.
(8) Rowan, A. E.; Nolte, R. J. M. *Angew. Chem., Int. Ed.* **1998**, *37*, 63.
(9) MacGillivray, L. R.; Atwood, J. L. *Nature* **1997**, *389*, 469.
(10) (a) Purrello, R.; Raudino, A.; Monsu Scolaro, L.; Loisi, A.; Bellacchio, E.; Lauceri, R. *J. Phys. Chem. B* **2000**, *104*, 10900. (b) Lauceri, R.; Raudino, A.; Monsù Scolaro, L.; Micali, N.; Purrello, R. *J. Am. Chem. Soc.* **2002**, *124*, 894. (c) Purrello, R.; Monsù Scolaro, L.; Bellacchio, E.; Gurrieri, S.; Romeo, A. *Inorg. Chem.* **1998**, *37*, 3647.
(11) Brittain, H. G., Ed. *Circular Dichroism Studies of the Optical Activity Induced in Achiral Molecules Through Association with Chiral Substances*; Elsevier: New York, 1994; Vol. 14.
(12) (a) Gibbs, E. J.; Tinoco, I.; Maestre, M. F.; Ellinas, P. A.; Pasternack, R. F. *Biochem. Biophys. Res. Commun.* **1988**, *157*, 350. (b) Pasternack, R. F.; Giannetto, A.; Pagano, P.; Gibbs, E. J. *J. Am. Chem. Soc.* **1991**, *113*, 7799.
(13) (a) Seifert, J. L.; Connor, R. E.; Kushon, S. A.; Wang, M.; Armitage, B. A. *J. Am. Chem. Soc.* **1999**, *121*, 2987. (b) Wang, M.; Silva, G. L.; Armitage, B. A. *J. Am. Chem. Soc.* **2000**, *122*, 9977.
(14) Chowdhury, A.; Wachsmann-Hogiu, S.; Bangal, P. R.; Raheem, I.; Peteanu, L. A. *J. Phys. Chem. B* **2001**, *105*, 12196.
(15) Kano, K.; Hasegawa, H. *J. Am. Chem. Soc.* **2001**, *123*, 10616.
(16) Allenmark, S. *Chirality* **2003**, *15*, 409.
(17) Pasternack, R. F.; Gibbs, E. J. In *Metal Ions in Biological Systems*; Siegel, A., Siegel, H., Eds.; Marcel Dekker: New York, 1996; Vol. 3.
(18) Lang, J.; Liu, M. *J. Phys. Chem. B* **1999**, *103*, 11393.
(19) Chen, X.; Liu, M. *J. Inorg. Biochem.* **2003**, *94*, 106.
(20) Lauceri, R.; Purrello, R.; Shetty, S. J.; Vicente, M. G. H. *J. Am. Chem. Soc.* **2001**, *123*, 5835.
(21) Wells, R. D.; Larson, J. E.; Grant, R. C.; Shortle, B. E.; Cantor, C. R. *J. Mol. Biol.* **1970**, *54*, 465.
(22) Yuan, J.; Liu, M. *J. Am. Chem. Soc.* **2003**, *125*, 5051.
(23) Spitz, C.; Dahne, S.; Ouart, A.; Abraham, H. W. *J. Phys. Chem. B* **2000**, *104*, 8664.
(24) Rubires, R.; Farrera, J.; Ribo, J. M. *Chem. Eur. J.* **2001**, *7*, 436.
(25) Maiti, N. C.; Mazumdar, S.; Periasamy, N. *J. Phys. Chem. B* **1998**, *102*, 1528.
(26) Ohno, O.; Kaizu, Y.; Kobayashi, H. *J. Chem. Phys.* **1993**, *99*, 4128.
(27) Choi, M. Y.; Pollard, J. A.; Webb, M. A.; McHale, J. L.; *J. Am. Chem. Soc.* **2003**, *125*, 810.
(28) (a) Akins, D. L.; Zhu, H. R.; Guo, C. *J. Phys. Chem.* **1996**, *100*, 5420. (b) Akins, D. L.; Zhu, H. R.; Guo, C. *J. Phys. Chem.* **1996**, *100*, 14390.
(29) Maiti, N. C.; Ravikanth, M.; Mazumdar, S.; Periasamy, N. *J. Phys. Chem.* **1995**, *99*, 17192.
(30) Koti, A. S. R.; Periasamy, N. *Chem. Mater.* **2003**, *15*, 369.
(31) Ribo, J. M.; Crusats, J.; Farrera, J. A.; Valero, M. L. *J. Chem. Soc. Chem. Commun.* **1994**, 681.
(32) Bellacchio, E.; Lauceri, R.; Gurrieri, S.; Scolaro, L. M.; Romeo, A.; Purrello, R. *J. Am. Chem. Soc.* **1998**, *120*, 12353.